THE EFFECT OF HOLD TIMES ON THE STRESS-STRAIN RELATIONSHIP FOR STEEL FIBER-REINFORCED REACTIVE POWDER CONCRETE AT ELEVATED TEMPERATURES

BAIFU LUO * **, YI LUO**
College of Civil Engineering and Mechanics, XiangTan University, XiangTan, China

With the purpose of further researching the fire-resistant performance of reactive powder concrete (RPC), the significant influence of hold times on the compressive stress versus strain relationship for RPC with 2% steel fibers (in volume) at elevated temperatures was investigated in this paper. Pursuing this objective, the experiment was performed at temperatures of 20 ℃, 200 ℃, 400 ℃, 600 ℃, and 800 ℃. In addition, axial compressive strength, elastic modulus, peak strain and energy absorption capacity (toughness) of RPC were evaluated at elevated temperatures. Furthermore, the compressive stress-strain constitutive equation was developed based on regression analysis. Results from the tests demonstrate that, with the increase of hold time, axial compressive strength of the RPC increases below 400 ℃, approximately decreases ranging from 400 ℃ to 600 ℃ and increases again at 800 ℃. At the temperature of 800 ℃, the elastic modulus (initial elastic modulus and peak secant modulus) and peak strain present adverse variation trends as the hold time increases. Moreover, the formula related to the initial elastic modulus and peak secant modulus was proposed.

Keywords: *Hold time; Elevated temperature; Reactive powder concrete; Stress-strain relation*

1. Introduction

Reactive powder concrete (RPC) that has ultra-high compressive strength and excellent durability is a new type of cement-based composite material. The cylindrical compression strength of RPC reached 200-800 MPa by mixing high-quality fine quartz sands, instead of traditional coarse aggregates, and curing under steaming or autoclaved conditions [1, 2]. On account of the above superior mechanical performances, RPCs have been widely applied to numerous engineering projects abroad, for example, bridges and maritime construction projects [3,4]. However, micron-size quartz sands and a low water-binder ratio result in a dense microstructure that makes RPC inferior at elevated temperatures compared with normal strength concrete (NSC) and high strength concrete (HSC). Stress-strain relationships, which are basic mathematical models for expressing the mechanical properties of concrete structures, are frequently applied to determine the fire resistance of concrete. Many relevant studies have been carried out on the stress-strain relationship for concrete at elevated temperatures [5, 6]. Chang et al. [7] indicated that the reductions of the elastic modulus, tensile strength, and compressive strength of NSC after exposure to temperature decreased consecutively, and in order. Cheng et al. [8] found that the aggregate type had a significant impact on the elastic modulus and ultimate strain of HSC at elevated temperatures. Liu et al. [9] acquired the residual stress-strain relationship for thermal insulation concrete and found that the elastic modulus decreased faster than the residual compressive strength. Tai et al. [10] found that the compressive peak strain of RPC decreased with the increase of temperature, but the peak stress increased. Zheng et al. [11,12] concluded that the elastic modulus was diminished more quickly than the compressive strength of steel fiber-reinforced RPC, after or under high temperature. Current research on the mechanical properties of concrete under high temperatures has only considered the mechanical performance under a steady state, but studies on the mechanical properties of concrete in which the internal and external temperature has reached a steady state, and kept for a period time, are rarely discussed. The hold time, that represents the length of time that this temperature is maintains after the core temperature of the specimen reaches the target temperature, is especially significant for the mechanical performance of concrete. This is because the behavior of fundamental components of concrete are especially affected by the increase of heating-up time. Chen et al. [13] found that there were significant differences on the ultimate strength and corresponding critical strain of normal weight concrete after the thermostatic sustaining time of 10 min or 20 minutes. He attributed this to the fact that the chemical reaction of different constituents in concrete is time-dependent. Moreover, Liang et al. [14] thought that the hold time also had an influence on RPC, but no further research was carried out. Additionally, relevant discussion was not found in the standards ISO 834-1-1999 (Fire-

* Autor corespondent/*Corresponding author*,
E-mail: luobaifu@gmail.com

resistance tests - Elements of building construction) [15]. To evaluate the fire-resistant performance of concrete more comprehensively, the influence of hold time (0 h, 1 h and 3 h) on compressive strength, peak strain, elastic modulus, toughness and stress-strain curves of RPC with 2% steel fibers (SRPC2) is investigated in this paper. Utilizing these experimental results, predictive equations were developed, and the proposed SRPC2 models were compared with the experimental results. Failure mode and expansive deformation of SRPC2 tests were also performed.

2. Experimental detail

2.1.Materials and mix proportion

SRPC2 was prepared by following ingredients: Grade 42.5 (Chinese cement grading system) ordinary Portland cement;silica fume (SF); blast-furnace slag (GGBS); fine quartz sand (0.212-0.42 mm) and crushed quartz powder (0.104-0.212 mm); polycarboxylate superplasticizer (SP); grade 60 brass-coated steel fibers with 0.22 mm diameters. The steel fibers are expressed as the percentage of concrete volume in the mixes. The mix proportions are summarized in Table 1. 45 prism specimens (70.7 × 70.7 × 220 mm) were prepared, and three specimens for each type were performed for all tests designed in this study.

2.2. Uniaxial compression test

The test furnace is of chamber size ϕ400×400 mm, with a maximum temperature of 1,200 ℃. Fig. 1 indicates the test furnace and loading device for the compressive test. Two special cylindrical alloy attachments (an upper heating and loading jig, and a bottom heating and loading jig) were added to the RPC specimens to transmit loads from the testing machine to the specimen, and to protect the test equipment. A K-type thermocouple was placed at the center of the test furnace to measure the furnace temperature. Mechanical tests were performed at a rate of 0.1 mm/min using a universal testing machine with a capacity of 5000 kN. Loads were recorded through a pressure sensor, using an automated computer controlled system. The complete stress-strain curves were obtained by high-strength steel alloy (U20452) rigid components (ϕ150×950 mm), to prevent premature end failure.

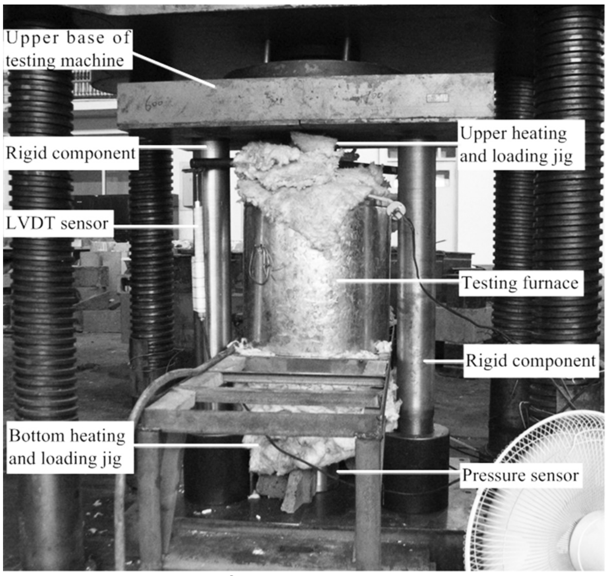

Fig.1 - Loading device for compressive test.

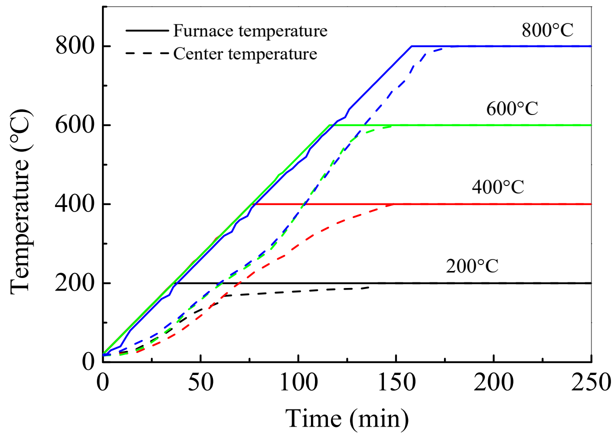

(a) Furnace and center temperature of SRPC2.

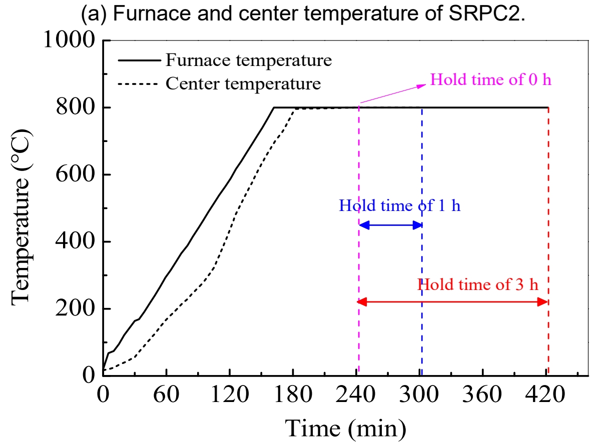

(b) Hold times at 800 ℃

Fig. 2. Temperature-time curves of the furnace and the specimen center and hold times at different target temperatures.

Table 1

RPC Test Mixtures

Mix	W/B	Binder			Quartz	SP	Steel fibers (%)
		C	SF	GGBS			
SRPC2	0.2	1	0.3	0.15	1.2	0.04	2

2.3. Heating regimes

The target temperatures of the test design were 20 °C, 200 °C, 400 °C, 600 °C and 800 °C. To avoid thermal spalling due to excess moisture, the heating rate was set at 5 °C/min. As shown in Fig. 2(a) and Fig. 2(b), each target temperature was maintained to achieve a thermal steady state, and the temperature was then maintained constant for an appointed time. In the case of the target temperature of 800 ℃，the hold time of h0 refers to the moment when the center temperature of the specimen and the furnace temperature are consistent at 800 ℃ (total time was 242 minutes). The hold times of h1 and h3 were hold 60 minutes and 180 minutes, respectively, using h0 as the baseline (the total times were 302 minutes and 422 minutes).

3. Results and discussion

3.1. Axial compressive strength

The compressive strength of SRPC2 at different hold times was presented in Fig. 3(a). When the temperature was below 400 ℃, the axial compressive strength of SRPC2-h3 was higher than that of SRPC2-h0 and SRPC2-h1 on account of high-pressure evaporation from free water failing to escape due to the dense microstructure of the RPC test specimen; furthermore, this induced an inner high-temperature and high-pressure curing environment or “internal autoclaving” [16]. Masdar et al. [17] have also recognized this advantageous effect. The compressive strength of SRPC2-h3 increased by 11% relative to SRPC2-h0 at 400 ℃. The compressive strength was augmented with the increase of the hold time, because the specimen manifested the effect of “self-steaming”, forming from the evaporation of bound water, and this effect further accelerated cement hydration and the pozzolanic reaction, creating more C-S-H gel. Concurrently, the C-S-H gel was transformed into xonotlite and tobermorite, which strengthened the compressive strength of the specimen [14]. The axial compressive strength of SRPC2 decreased with the increase of hold time when the heating temperature was between 400 ℃ and 600 ℃. The main reason is that there are cracks and holes resulting from the decomposition of CH [18], and cubical dilatation on account of the transformation of quartz sands [19]. In other words, cracks and holes became more prevalent with the increase of hold time. However, the axial compressive strength of SRPC2-h0, SRPC2-h1 and SRPC2-h3 was respectively 28.34 MPa, 38.67 MPa and 52.95 MPa at 800 ℃, and the compressive strength of SRPC2-h3 increased by 86.8% relative to SRPC2-h0. This signifies that the axial compressive strength increased with the increase of hold time at the temperature of 800 ℃, which can be attributed to the sintering of cement paste.

In addition, the normalized compressive strength of SPRC2 of different hold times at elevated temperatures as a function of temperature, proposed by the EN 1994-1-2 (CEN 2004) and ACI 216 (ACI 1989) codes, was also given in Fig. 3(b). Obviously, it is seen that the codes of EN 1994-1-2 (CEN 2004) and ACI 216 (ACI 1989) overestimate the experimental normalized compressive strength results of SRPC2 for different hold times below 600 °C.

Following regression analysis, the relationship of the relative axial compressive strength with the temperature T is given by Eq. (1). It can be seen from Fig. 3(b) that the proposed model fits the experimental data well.

$$\frac{f_{c,T}}{f_{c,20}} = 1.01 - 0.96\left(\frac{T}{1000}\right),\ 20°C \le T \le 800°C,\ R^2 = 0.981 \tag{1}$$

where $f_{c,T}$ and $f_{c,20}$ are respectively the compressive strength at the target temperature and normal temperature; T is the heating temperature; R^2 is the correlation coefficient.

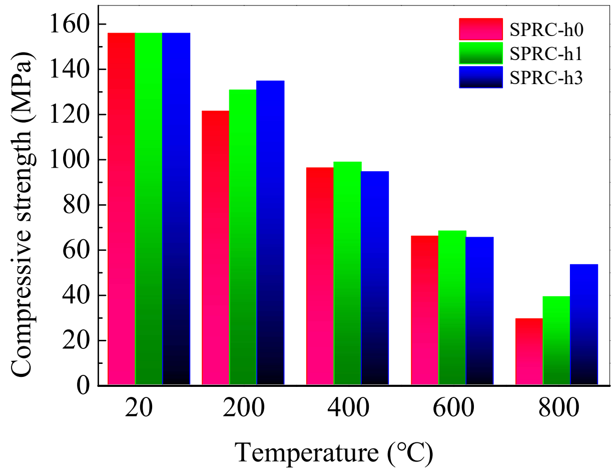

(a) absolute value

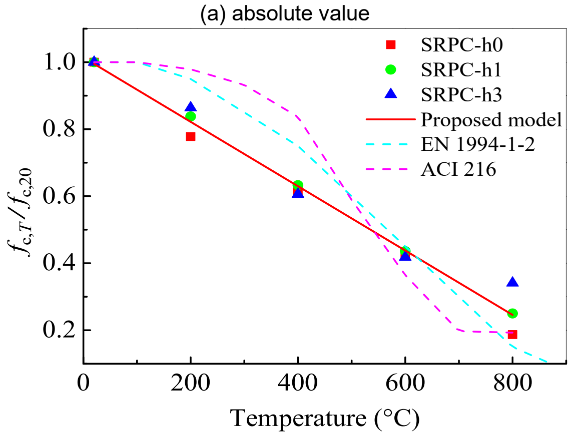

(b) relative value

Fig. 3 - The effect of hold time on compressive strengths of SRPC2.

3.2. Development of the stress-strain relationship

3.2.1. Elastic modulus

Initial elastic modulus E_{oT} (the secant modulus at 0.5 $f_{c,T}$) and peak secant modulus E_{pT} (the secant of modulus at $f_{c,T}$) of SRPC2 at different hold times, varying with the temperature, at high temperatures, were plotted in Fig. 4(a) and Fig. 4(b). The initial elastic modulus and peak secant modulus of SRPC2 at different hold times decreased with increasing temperature, but increased when the temperature was 800 ℃. The initial elastic modulus of SRPC2-h3 at the temperatures of 200 ℃, 400 ℃, 600 ℃ and 800 ℃ was, respectively, 47.4%, 25.4%, 14.0% and 14.1% of that at 20 ℃. The initial elastic modulus went up slightly at 800 ℃, which was similar to the change regulations of compressive strength. When the heating temperature was between 20 ℃ to 600 ℃, the initial elastic modulus of SRPC2 under different hold times was less than that of the ASCE manual [20] and Sanchayan [21] , but higher than that of EN 1994-1-2 [22]. However, the initial elastic modulus of SRPC2-h1 and SRPC2-h3 reached its maximum at 800 ℃.

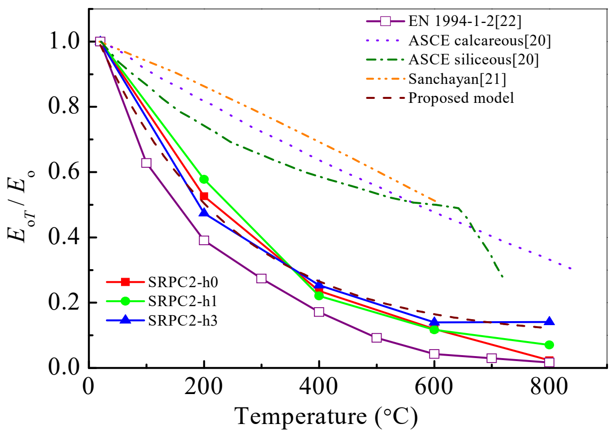

initial elastic modulus

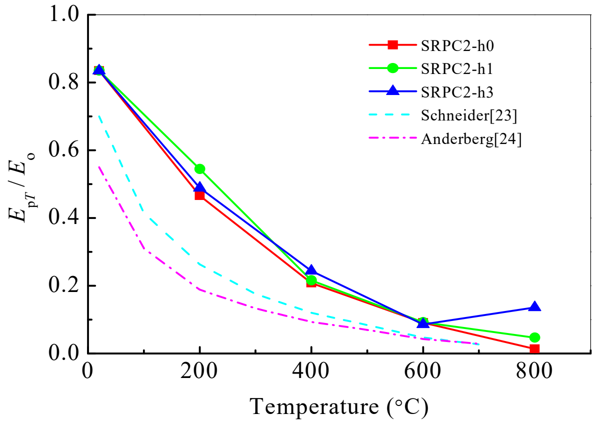

(b) peak secant modulus

Fig. 4 - Elastic modulus of SRPC2 for different hold times at elevated temperatures.

The peak secant modulus of SRPC2 at different hold times lost 50.03% on average at 200 ℃. However, the studies of Schneider [23] and Anderberg [24] demonstrate that the peak secant modulus lost 75% more when the temperature was 200 ℃. Moreover, the peak secant modulus of SRPC2-h1 and SRPC2-h3 were higher than that of Schneider [23] and Anderberg [24] at 800 ℃. The primary cause is that the cement mortar sintered and then the compressive strength rose with the increase of hold time. Moreover, the regulation of increase for the modulus and compressive strength was similar.

Through representation, the correlation coefficient of the fitting precision is $R^2 = 9.959$. The change of E_{oT}/E_o and E_{pT}/E_p corresponding to SRPC2 at different hold times varying with temperature was expressing below.

$$\frac{E_{oT}}{E_o} = \frac{E_{pT}}{E_p} = 0.091 + 0.979\exp(-0.00371T) \tag{2}$$

E_{oT} and E_{pT} are respectively the initial elastic modulus and the peak secant modulus of SRPC2 for different hold times at the heating temperature, E_o and E_p are respectively the initial elastic modulus and the peak secant modulus at the normal temperature, T is the value of the temperature at the heating temperature.

3.2.2. Peak strain

As shown in Fig. 5(a), the peak strain of SRPC2 was increasing with the temperature increasing. When the temperature was 200 ℃, 400 ℃ and 600 ℃, the peak strain of SRPC2-h0, SRPC2-h1 and SRPC2-h3 was similar, and the average values were, respectively, 5.62×10^3, 10.02×10^3 and 14.51×10^3. However, the peak strain of SPRC2 at different hold times varied greatly at 800℃, and was variously 55.31×10^3, 19.71×10^3 and 9.93×10^3. The peak strain of SRPC2-h1 and SRPC2-h3 respectively decreased by 64.3% and 82.05% relative to that of SPRC2-h0 at 800 ℃.

The variation rule of temperature and ratio ($\varepsilon_{c,T}/\varepsilon_o$) between the peak strain of SRPC2 for different hold times at the elevated temperature was shown in Fig. 5(b). The peak strain of SRPC2 at different hold times is higher than that of Lu [25], but less than that of EN 1994-1-2 [22], in addition to the temperature of 800 ℃. The peak strain obviously increased beyond 600 ℃, because the CH and C-S-H decomposed [16], a mass of cracks was produced, and the effective area of compression reduced. However, the peak strain decreased as the hold time increased at 800 ℃, due to the fact that the sintering of cement mortar

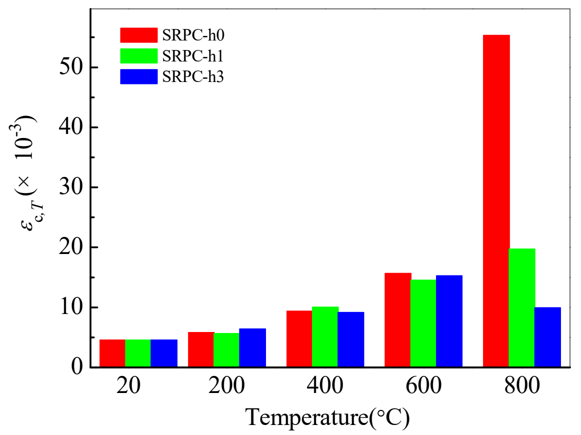

(a) absolute value

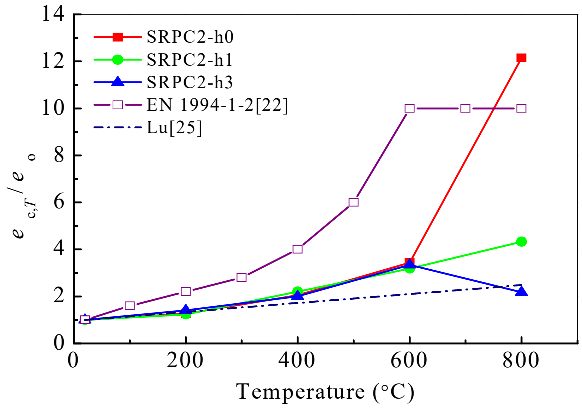

(b) relative value

Fig. 5 - Peak strain of SRPC2 for different hold times.

was more effective, the outer concrete of the specimen was more dense, and the number of holes reduced, resulting in higher compressive strength. Therefore, the peak strain of SRPC decreases with the increase of hold time, and the reduction of peak strain mainly results from the decrease of holes and cracks with the increase of hold time.

3.2.3. Energy absorption capacity (toughness)

The energy absorption capacity, or toughness, of concrete in compression has been defined as the area under the stress–strain curve calculated up to a specified strain value. The toughness of SRPC2 of different hold times at elevated temperatures was shown in Fig. 6. The toughness of SRPC2-h0, SPRC2-h1 and SRPC2-h3 increased in turn at the temperature of 200 ℃, and the toughness increased with the increase of hold time. When the temperature was 400 ℃ and 600 ℃, the toughness of SRPC2-h0 was higher than that of SPRC2-h1 and SRPC2-h3, and the toughness reduced with the increase of hold time, because of holes and cracks resulting from the evaporation of the bound water. The toughness of SRPC2-h0, SPRC2-h1 and SRPC2-h3 was, respectively, 1441.65, 777.88 and 540.59, at 800 ℃, and the toughness reduced in turn with the increase of hold time. The compressive strength increased with the increase of hold time while the strain decreased sharply at the same time, and the area under the stress-strain curve also decreased, resulting in the final reduction of the toughness.

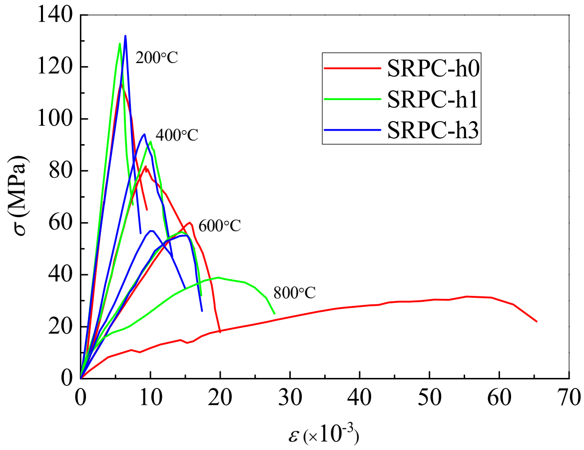

Fig. 6 - Energy absorption capacity of SRPC2 for different hold times

3.2.4. Compressive stress-strain curves

The compressive stress-strain curves, corresponding to high temperatures, of SRPC2-h0, SRPC2-h1 and SRPC2-h3 were shown in Fig. 7. As the temperature increases, the compressive strength decreases, the peak strain increases and the elastic modulus decreases sharply for SRPC2-h0, SRPC2-h1 and SRPC2-h3. Therefore, the elastic modulus of SRPC at different hold time decreases with the increase of temperature, but the peak strain increases. In addition, with the increase of temperature, the compressive stress-strain curve tends to be gentle, and the non-linearity of the ascending section also increases. When the heating temperature was between 20 ℃ to 400 ℃, the peak strain of SRPC2-h1 and SRPC2-h3 was significantly augmented relative to SRPC2-h0. However, the peak strain of SRPC2-h1 and SRPC2-h3 was obviously smaller than SRPC2-h0 at 800 ℃. The reason is the decomposition of CH and C-S-H at elevated temperatures [16], and the fact that the thermal expansion coefficient of quartz sand and cement mortar is not consistent at 800℃ [26].

3.2.5. Suggestion of the mode equation

For the compressive stress-strain curves of concrete, domestic and foreign scholars have put forward many different kinds of uniaxial compressive stress-strain curves [27]. Some of these equations adopt the uniform equation of the ascending and descending section curves, but some of them are piecewise equations, and their functions are polynomial, exponential, trigonometric and rational. Guo [30] used the polynomial and rational fraction to fit the model according to the shape of the ascending and the descending section curves from the whole curve.

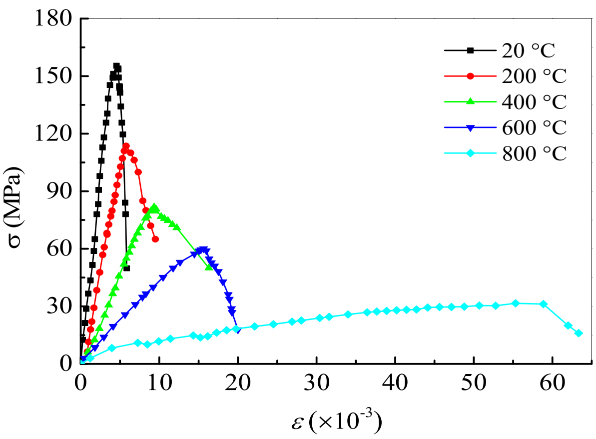

(a) SRPC2-h0

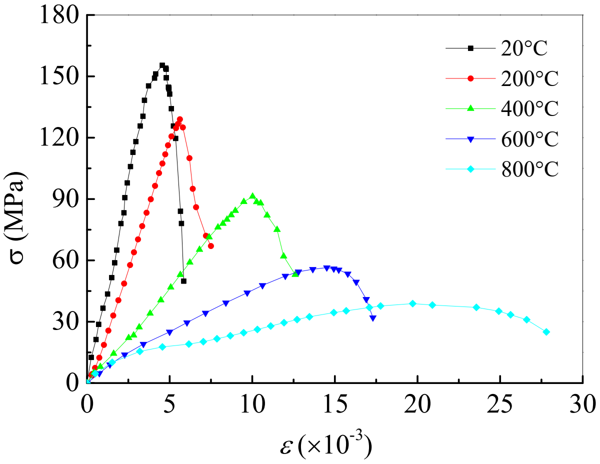

(b) SRPC2-h1

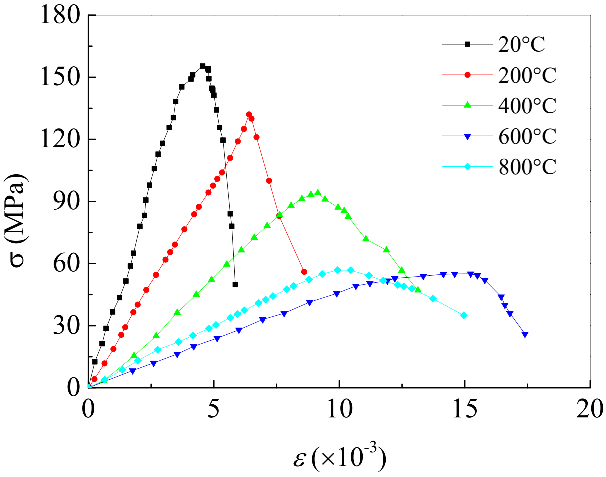

(c) SRPC2-h3

Fig. 7- Compressive stress-strain curves of SRPC2 for different hold times.

Because the model is consistent with the continuous curve at the peak point, and the parameters in the equation can be adjusted to meet the curve shape of different concrete materials, it belongs to the refined model. This paper further developed Guo's model equation through modifying the parameter of λ and μ in Eq. (3).

λ and μ are two independent parameters controlling the ascending and descending sections of the stress-strain curve. Through regression analysis and programming, the specific parameter values λ and μ can be calculated, which are shown in Table 2. After λ and μ were respectively substituted into Eq. (3), the theoretical curve could be acquired. The theoretical curve and test results were shown in Fig. 8, which are in good agreement. λ scales linearly for increases in temperature from 200 ℃ to 800 ℃ and the nonlinearity of the ascending curves adds with the increasing temperature. When the temperature increases ranging from 200 ℃ to 800 ℃, μ decreases and the area under the descending curves reduces, except for 600 ℃.

Table 2

Equation parameters of SRPC2 for different hold times

Temperature		200℃	400℃	600℃	800℃
Parameter	λ	1.05	1.07	1.25	1.43
	μ	11	6	13	5

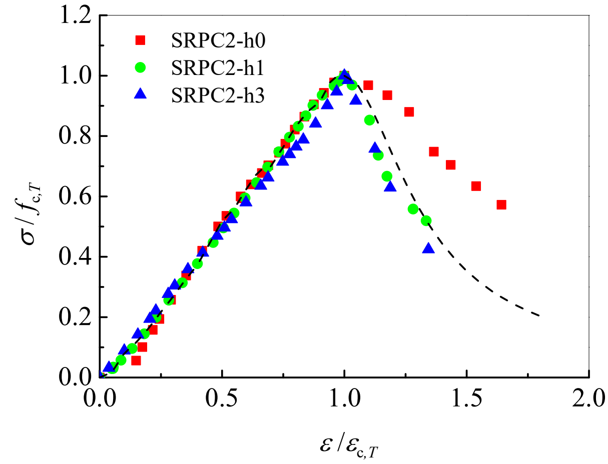

(a) 200 ℃

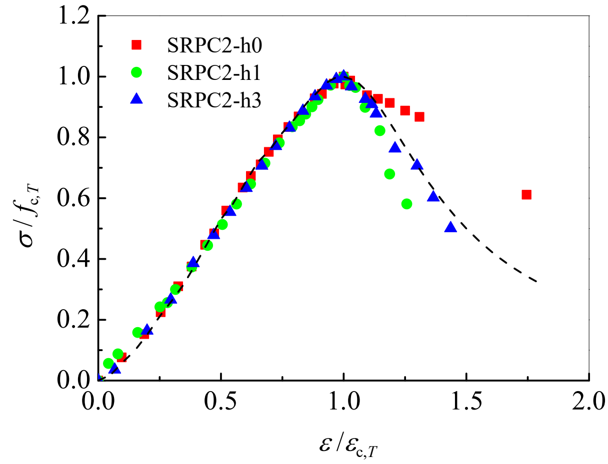

(b) 400 ℃

Fig. 8 continues on next page

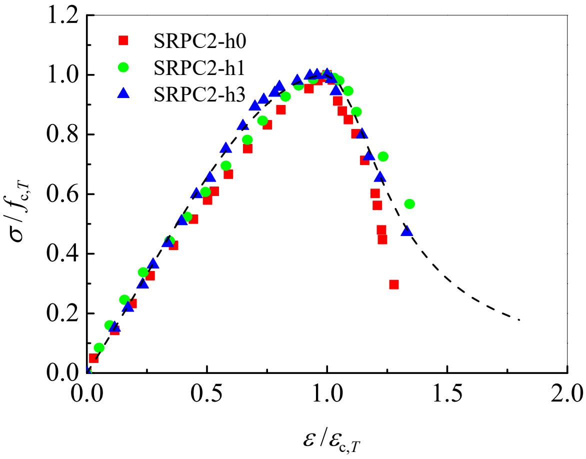

(c) 600 ℃

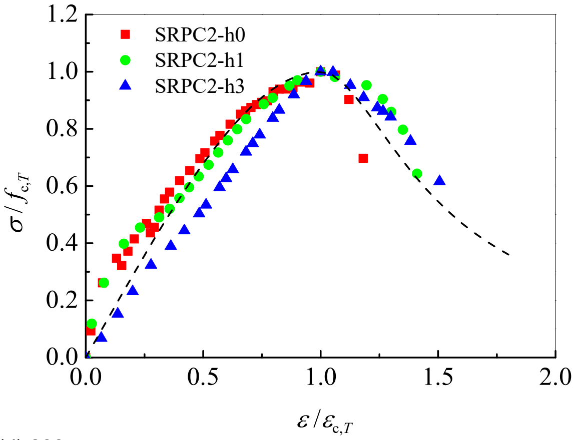

(d) 800 ℃

Fig. 8 - Stress–strain fitting curves of SRPC2 for different hold times.

$$y=\begin{cases}\lambda x+(3-2\lambda)x^2+(\lambda-2)x^3, & 0\le x\le 1;\\ \dfrac{x}{\mu(x-1)^2+x}, & x>1.\end{cases} \qquad (3)$$

where y equals $\sigma/f_{c,T}$ and x equals $\varepsilon/\varepsilon_{c,T}$, σ and ε are, respectively, stress and strain of compression, $f_{c,T}$ and $\varepsilon_{c,T}$ are, respectively, axial compressive strength and peak strain.

3.2.6. Verification of the proposed model equation

Through analyzing the λ and μ parameters of Eq. (3), the stress-strain full curve of RPC with steel fibers for different hold times can be acquired. The theoretical curves were compared with the experimental results at different temperatures in order to verify the proposed model. It can be seen from Fig. 9 that the proposed model of SRPC2-h0, SRPC2-h1 and SRPC2-h3 is more consistent with the whole curve of the experimental results by comparison with the Mander model [31].

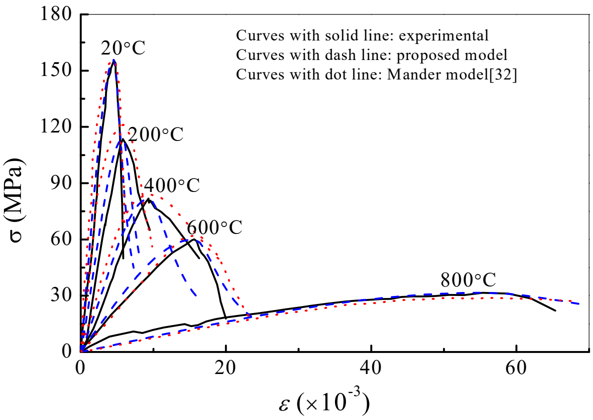

(a) SRPC2-h0

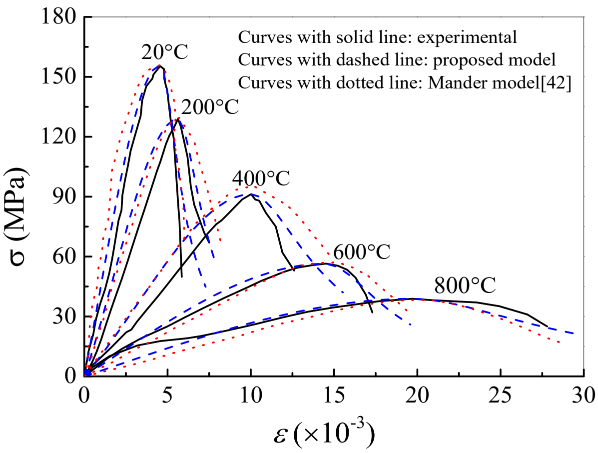

(b) SRPC2-h1

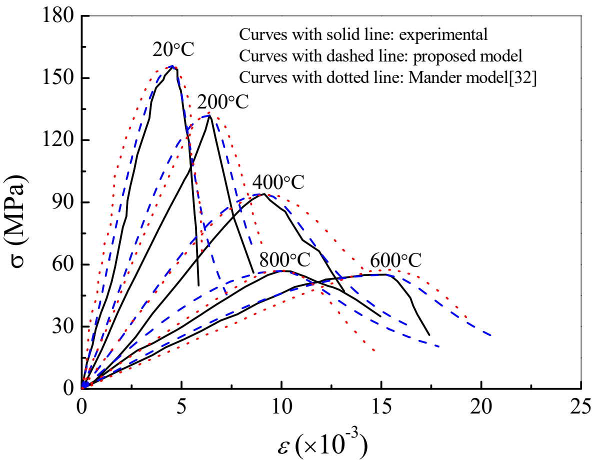

(c) SRPC2-h3

Fig. 9 - Comparison of proposed stress-strain curves with experimental results for SRPC2 for different hold times at elevated temperatures.

4. Conclusions

Through the analysis of the above experimental results, the following conclusions related to the mechanical performance and the hold time of RPC with 2% steel fibers at elevated temperatures can be drawn:

(1) The variation of axial compressive strength of SRPC2 for different hold times at the target temperature divided approximately into three phases: the axial compressive strength of SRPC2 increased at temperatures below 400 ℃, decreased at the temperatures from 400 ℃ to 600 ℃, and again increased at 800 ℃ with the increasing hold time. It can be confirmed that the strength of RPC with 2% steel fibers changes as the hold time increases.

(2) For different hold times, the initial elastic modulus and peak secant modulus of SRPC2 decreased as the temperature increased, while that of SRPC2 increased as the hold time increased at 800 ℃. Further, the peak strain of SRPC2-h0, SRPC2-h1 and SRPC2-h3 had little difference at temperatures below 600 ℃, but there were some differences at the temperature of 800 ℃. Based on experimental data, a computational formula to calculate the modulus by temperature was established. The energy absorption capacity of SRPC2 heightened as the hold time increased at the temperature of 200 ℃; and reduced beyond 400 ℃.

(3) For SRPC2-h0, SRPC2-h1 and SRPC2-h3, the whole stress-strain relationship curve tended to flatten, and the descending section of the curve became non-linear with the increase of temperature. According to the compressive stress-strain curves of the experimental results, the piecewise equation which controls the shape of the compressive stress-strain curves was developed by defining parameters. From the proposed model, the compressive stress-strain curves of SRPC2 for different hold times and some mechanical performances (such as compressive strength, elastic modulus or peak strain) can be indicated.

(4) It was unsafe when the EN 1994-1-2 and ACI 216 were used for estimating the compressive strength of SRPC2 of different hold times below 600 °C, while the EN 1994-1-2 gave an overestimation for the peak strain at all temperatures.

Acknowledgements

Financial support from Research Foundation of Education Bureau of Hunan Province, China (15C1329), Innovative Venture Technology Investment Project of Hunan Province (2018GK5028) are gratefully acknowledged.

REFERENCES

[1] P. Richard, M. Cheyrezy. Reactive powder concretes with high ductility and 200-800 MPa compressive strength[J]. ACI Special Publication, 1994, **144**(24), 507-518.

[2] P. Richard, M. Cheyrezy. Composition of reactive powder concretes[J]. Cement and Concrete Research, 1995, **25**(7), 1501-1511.

[3] B. Cavil, G. Chrigwin. The world’s first ductal road bridge at Shepherds Gully Greek Bridge[C] // CIA 21th Biennial Conference. Brisbane, Queensland: Australian Road Research Board, 2003, 1-11.

[4] M. Cheyrezy. Structural Application of RPC[J]. Concrete, 1999, **33**(1), 20-23.

[5] L. Y. Li, J. Purkiss. Stress-strain constitutive equations of concrete material at elevated temperatures[J]. Fire Safety Journal, 2005, **40**, 669-686.

[6] M.A. Youssef, M. Moftah. General stress-strain relationship for concrete at elevated temperatures[J]. Engineering Structures, 2007, **29,** 2618-2634.

[7] Y. F. Chang, Y. H. Chen, M. S. Sheu et al. Residual stress-strain relationship for concrete after exposure to high temperatures[J]. Cement and Concrete Research, 2006, **36**, 1999-2005.

[8] F. P. Cheng, V. K. R. Kodur, T. C. Wang. Stress-strain curves for high strength concrete at elevated temperatures[J]. Journal of Materials in Civil Engineering, 2004, **16**, 84-90.

[9] Y. Z. Liu, W. J. Wang, Y. F. Chen, et al. Residual stress-strain relationship for thermal insulation concrete with recycled aggregate after high temperature exposure[J]. Construction and Building Materials, 2016, **129**, 37-47.

[10] Y. S. Tai, H. H. Pan, Y. N. Kung. Mechanical properties of steel fibre reinforced reactive powder concrete following exposure to high temperature reaching 800 ℃[J]. Nuclear Engineering and Design, 2011, **241** (7), 2416-2424.

[11] W. Z. Zheng, H. Y. Li, Y. Wang. Compressive stress-strain relationship of steel fiber-reinforced reactive powder concrete after exposure to elevated temperatures[J]. Construction and Building Materials, 2012, **35**, 931-940.

[12] W. Z. Zheng, B. F. Luo, Y. Wang. Stress-strain relationship of steel-fibre reinforced reactive powder concrete at elevated temperatures[J]. Materials and Structures, 2015, **48**(7), 2299-2314.

[13] L. Chen, Q. Fang, X. Jiang, et al. Combined effects of high temperature and high strain rate on normal weight concrete[J]. Internal Journal of Impact Engineering. 2015, **86**, 40-56.

[14] X. W. Liang, C. Q. Wu, Y. Su, et al. Development of ultra-high performance concrete with high fire resistance[J]. Construction and Building Materials. 2018, **179**, 400-412.

[15] ISO 834-1-1999 (E), Fire-resistance tests - Elements of building construction - Part 1: General requirements, International Organization for Standardization, Geveve, 1999.

[16] A. M. Rashad, Y. Bai, P. A. M. Basheer, et al. Chemical and mechanical stability of sodium sulfate activated slag after exposure to elevated temperature[J]. Cement and Concrete Research. 2012, **42**(2), 333-343.

[17] M. Helmi, M. R. Hall, L. A. Stevens, et al. Effects of high-pressure/temperature curing on reactive powder concrete microstructure formation[J]. Construction and Building Materials. 2016, **105**, 554-562.

[18] S. Y. N. Chan, G. F. Peng, M. Anson. Residual strength and pore structure of high-strength concrete and normal-strength concrete after exposure to high temperatures[J]. Cement and Concrete Composites, 1999, **21**(1), 23–27.

[19] T. Uygunoğlu, İ. B. Topçu. Thermal expansion of self-consolidating normal and lightweight aggregate concrete at elevated temperature[J]. Construction and Building Materials, 2009, **23**(9), 3063-3069.

[20] American Society of Civil Engineers (ASCE), Structural Fire Protection. Committee on Fire Protection, Structural Division, ASCE, New York, NY, USA, 1992.

[21] S. Sanchayan, S. J. Foster. High temperature behaviour of hybrid steel-PVA fibre reinforced reactive powder concrete, Materials and Structures, 2016, **49**(3), 769-782.

[22] British Standards Institution. EN. 1994-1-2:2005 Eurocode 4: Design of Composite Steel and Concrete Structures-Part1.2: General Rules–structural Fire Design [S]. London: British Standards Institution, 2005.

[23] U. Schneider. Modelling of concrete behaviour at high temperatures[C]. In: Anchor, R. D., Malhotra, H. L., Purkiss, J.A, Proceeding of international conference of design of structures against fire, 1986.

[24] Y. Anderberg, S. Thelandersson. Stress and deformation characteristics of concrete at high temperatures: 2 experimental investigation and material behaviour model. Bulletin 54[C]. Sweden (Lund): Lund Institute of Technology, 1976.
[25] Z. D. Lu. Study on fire response of reinforced concrete beams[D]. Tongji University Institution of Engineering Structure, 1989.(in Chinese)
[26] W. Khaliq, V. Kodur. Thermal and mechanical properties of fiber reinforced high performance self-consolidating concrete at elevated temperatures[J]. Cement and Concrete Research, 2011, **41**(11), 1112–1122.
[27] British Standards Institution. EN. 1992-1-2:2004 Eurocode 2: Design of Concrete Structures-Part 1.2: General Rules-Structural Fire Design[S]. London: British Standards Institution, 2004.
[28] H. T. Hu, L.Y. Dong. Experimental research on strength and deformation of high-strength concrete at elevated temperatures[J]. China Civil Engineering Journal, 2002, **35**(6), 44-47.
[29] V. K. R. Kodur, T. C. Wang, F. P. Cheng. Predicting the Fire Resistance Behavior of High Strength Concrete Columns[J]. Cement & Concrete Composites, 2004, **26**(2), 425-430.
[30] Z. H. Guo, X. D. Shi. Thermal performance and compute of reinforced concrete[M]. Beijing: Press of Tsinghua University, 2003, 73-76.
[31] J. B. Mander, M. J. N. Priestley, R. Park. Theoretical stress-strain model for confined concrete[J]. Journal of Structural Division, ASCE. 1988, **114**(8), 1804-1826.

****